Available online at www.sciencedirect.com
ScienceDirect
Journal of the European Ceramic Society 30 (2010) 1445–1452
www.elsevier.com/locate/jeurceramsoc

In situ measurement of material properties of lead zirconate titanate piezoelectric ceramics during cyclic mechanical loading

Mitsuhiro Okayasu *, Eriko Sugiyama, Mamoru Mizuno

Department of Machine Intelligence and Systems Engineering, Akita Prefectural University, 84-4 Ebinokuchi, Tuchiya-aza, Yurihonjo-city, Akita 015-0055, Japan

Received 8 May 2009; received in revised form 23 October 2009; accepted 4 November 2009
Available online 8 December 2009

Abstract

To better understand the material properties of lead zirconate titanate (PZT) ceramics, in situ mechanical and electrical properties have been investigated continuously during cyclic mechanical loading. The material properties are demonstrated to change as a function of applied maximum stress, with the effective elastic constant increasing with increase of the stress level. The increase of effective elastic constant is attributed to the domain structure of the PZT. 90° domain switching can occur anywhere in the sample, which makes the strain accumulate and leads to high values of the effective elastic constant. The domain switching characteristics are clearly revealed by electron back scattered diffraction analysis. The changes of the electrical properties (electromechanical coupling coefficient, piezoelectric constant and permittivity) are in the opposite sense because of the material strain (or material damage), caused by the change of domain orientation; the electrical properties are degraded with increasing cycle number and applied stress. Based upon the variation of the material properties, details of the damage characteristics in the PZT ceramics are discussed.

Keywords: PZT ceramic; Electroplate; Domain switching; Fatigue strength; Mechanical property

1. Introduction

In recent years, piezoelectric ceramics have offered promising applications in many smart structures. In particular, the ceramic material lead zirconate titanate (PZT) is employed in a number of actuator applications including precision positioning. Recent demands on actuators in smart structures are that these materials perform under increasingly high electric and mechanical loads. Thus, the durability and reliability of actuators are significant factors in their use over long periods of time [1]. An experimental investigation has been performed into the fatigue properties of PZT ceramic under electrical and mechanical loads. The experimental approach to fatigue has involved characterization of the crack growth characteristics, i.e., da/dN–ΔK relationship, and the total life to failure in terms of a cyclic stress range, i.e., the S–N relationship. Those approaches include an estimate of the number of cycles required to induce final failure. Until now, the effects of material properties on the fatigue strength in PZT ceramics have been investigated by many researchers [2–4]. In our previous works [3], the fatigue properties are influenced by the status of the electrode attached to the PZT ceramic, e.g., (i) the surface roughness of the electrode and (ii) the penetration of the electrode material into the substrate. In order to understand the material properties of PZT during applied loading, an examination of the damage characteristics in PZT during cyclic loading has been conducted. There are several damage characteristics in the PZT: material failure and domain switching (polarization). In the study by Cheng et al. [4], compression fatigue tests were performed using PZT ceramics. Their results show that small compression loadings induce large detrimental cracks. Additional work is in progress to model the deformations at the crack tip and consequent generation of residual tensile stresses to predict the growth of damage and cracks in PZT ceramics. Domain switching characteristics in piezoelectric ceramics have been examined by several researchers. Jones et al. and Pojprapai et al. have examined the domain switching characteristic using neutron diffraction [5], and it appeared that macroscopic strain

* Corresponding author.
E-mail address: okayasu@akita-pu.ac.jp (M. Okayasu).

0955-2219/$ – see front matter © 2009 Elsevier Ltd. All rights reserved.
doi:10.1016/j.jeurceramsoc.2009.11.004

is composed of two components [6]: the intrinsic lattice strain and the strain resulting from ferroelastic domain switching. The domain switching phenomenon under electromechanical loading has been investigated in situ with polarized light microscopy [7], where it appeared that a 90° domain switching zone is apparent near the crack tip and that the size of the switching zone changed with the sharpness of the crack tip. Kreher [8] has proposed a fracture model for ferroelectric materials taking into account the hysteretic domain switching processes near the tip of a macroscopic crack. The model is based on the balance of energy supplied by the driving forces, and the total energies either dissipated by domain switching, stored in the crack wake region or consumed by the formation of new fracture surfaces. Because the above material damage in the PZT ceramics, e.g., domain switching, can be attributed to crack growth characteristics, this type of damage could also affect the material properties, such as electromechanical coupling coefficient and piezoelectric constant. Several investigators have examined the electrical properties of PZT ceramics at various temperatures [9]. However, there appears to be little information about those properties during the mechanical loading. Such information is especially significant for the design of PZT devices [10]. Moreover, whereas the material strength of PZT ceramics is relatively well understood, details of domain switching characteristics under applied loading have not been reported clearly. To observe the domain orientation, several experimental techniques have been utilized, including etching techniques [11], X-ray diffraction [5,12] and scanning force microscopy [13]. In recent years, some researchers have employed electron back scattered diffraction (EBSD) to reveal clearly the crystal orientation in various metals, such as pure aluminum [14], 2014 aluminum alloy [15] and copper [16]. Although the EBSD technique clearly reveals crystal orientation, this technique is seldom used for research into PZT ceramics. The main purpose of this paper is, therefore, to investigate the domain structure of PZT during the loading process using EBSD analysis. In addition, in situ measurements of the material properties of PZT during cyclic loading have been carried out to understand clearly the relationship between the material damage and material properties.

2. Experimental procedures

2.1. Materials

The soft piezoceramic chosen for the present work was a commercial bulk lead zirconate titanate ceramic ($PbZrTiO_3$), produced by Fuji Ceramics Co. in Japan. The nominal grain size of this ceramic is about 5 μm. The PZT ceramics adopt a tetragonal perovskite structure with $a = b = 0.4046$ nm and $c = 0.4103$ nm at room temperature. The aspect ratio c/a, determined by X-ray diffraction (XRD), is about 1.014. In the present work, rectangular rod specimens with dimension 2.7 mm × 2.7 mm × 7.5 mm were employed. The bulk PZT sample was produced by the following process: (i) PZT powder with grain size 5 μm is piled together with a binder in a mold at about 175 MPa before firing in atmosphere at 1200 °C; (ii) silver powder was coated on to two opposite sides of the PZT surfaces; (iii) the silver-based electroplating was attached to the sample surfaces and fired in atmosphere at 700 °C for several hours; (iv) after the electrode attachment, the samples were immersed in silicon oil and electrically poled using electric fields at 2 kV/mm. Note that the thickness of the silver electrode was approximately 10 μm. Fig. 1 shows a schematic illustration of the specimens. In this work, samples with different poling directions were used to examine (i) the effect of the poling direction (Sample A vs. Sample B) and (ii) the effect of sample thickness (Sample B vs. Sample C) on the material properties. Note that the specimens were all produced from the same production lot, ensuring similar material quality.

2.2. Experiments

The compression tests were performed on the PZT ceramics using a screw driven type universal testing machine with 10 kN capacity (Shimadzu EZGraph). The resolutions of load and displacement in this testing machine are 0.01 N and 1 μm, respectively. The loading speed for the compression tests was 1 mm/min to final fracture. The fatigue test was also conducted with compression–compression mechanical loads at a frequency of 0.05 Hz and R ratio of 0.05. The maximum mechanical cyclic stress, σ_{max}, was determined on the basis of the compression strength (σ_B), where σ_{max} is designed to be less than 90% of σ_B. The compression loads were applied along the direction normal to the electrode surface (Sample A: $P \perp E$) or parallel to the electrode (Sample B and Sample C: $P // E$) (see Fig. 1). It should be mentioned that (i) the load was applied to the entire surface of the PZT specimen to prevent shear failure and (ii) in the fatigue tests a low measurement frequency was employed to reduce mechanical damage in the sample. The electrical properties of the PZT ceramics were examined during the mechanical loading process, e.g., the electromechanical coupling coefficient, k_{33}, and piezoelectric constant, d_{33}. Those properties were obtained from the anti-resonance frequency f_a, resonance frequency f_r and electrostatic capacity C^T of the samples measured by an impedance analyzer (Agilent Technologies, 4294A). With f_a and f_r values, k_{33} can be calculated [17,18]:

$$k_{33} = \sqrt{\frac{1}{a(f_r/(f_a - f_r)) + b}} \tag{1}$$

where a and b are the coefficients for each vibration mode. On the other hand, the piezoelectric constant, d_{33}, can be determined from the following formula:

$$d_{33} = k_{33}\sqrt{\frac{\varepsilon_{33}}{c_{33}^E}} \tag{2}$$

where ε_{33} and c_{33}^E are the permittivity and elastic coefficient, respectively. In this case, both parameters are expressed as:

$$\varepsilon_{33} = \frac{C^T t}{A} \tag{2a}$$

$$c_{33}^E = (2lf_r)^2\rho \tag{2b}$$

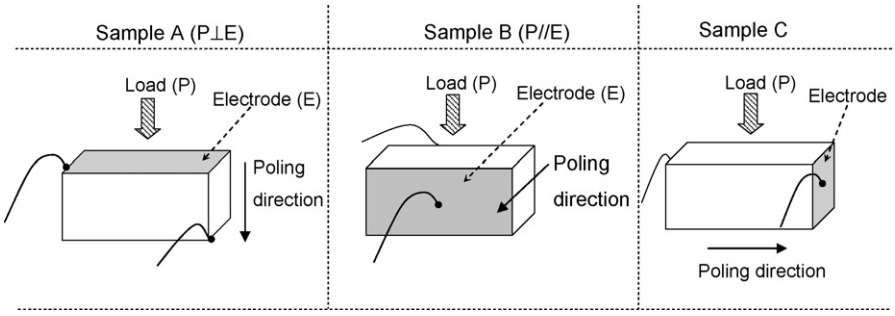

Fig. 1. Schematic illustration of the rectangular rod specimens used for compressive loading.

Table 1
Material properties of the PZT ceramics.

Elastic constant c_{33}^E	Electromechanical coupling coefficient (k_{33})	Piezoelectric constant (d_{33})	Permittivity (ε_{33})	Dielectric constant ($\varepsilon_{33}/\varepsilon_0$)
37 GPa	0.76	533 pm/V	20.5 nF/m	2260

where t is the distance between the two electrodes and A is the area of the electrode. l and ρ represent the length of the specimen and the density of PZT, respectively. Details of the above calculations can be found in Refs. [17,18]. The material properties of the PZT ceramics after polarization were examined before the experiments. Table 1 indicates the material properties of the PZT used in the present work: (i) effective elastic constant (c_{33}^E) 37 GPa, (ii) electromechanical coupling coefficient (k_{33}) 0.76, (iii) piezoelectric constant (d_{33}) 533 pm/V and (iv) permittivity (ε_{33}) 20.5 nF/m (or dielectric constant ($\varepsilon_{33}/\varepsilon_0$) 2260). The anti-resonance frequency f_a of this PZT ceramic is approximately 2.32×10^5 Hz.

2.3. Domain structure

In the present work, an attempt was made to observe the domain structure (crystal orientation and domain wall) before and after applied load by electron back scatter diffraction (EBSD) analysis. This analysis was conducted using high resolution electron microscopy (JEOL JEM-200EX) with an orientation imaging microscopy system. In this examination, the sample surface for the observation was first polished to a mirror finish using colloidal silica. The sample surfaces were then coated with carbon. Details of the EBSD technique are summarized by Randle [19].

3. Results and discussion

3.1. Stress–strain relations

Fig. 2 shows the relationship between the compressive stress (σ_c) and strain (ε_c) for both rectangular samples (Samples A and B). In the 1st cycle, nonlinear stress–strain curves are obtained and the strain level increases sharply in the beginning of the 1st cycle. On the other hand, the σ_c vs. ε_c relationship shows a similar pattern following the 2nd cycle in both samples. Similar σ_c vs. ε_c relationships have been obtained in earlier studies by several researchers [20–22]. In this case, such a large strain in the 1st cycle can be a result of domain switching, i.e., in the unloading process, some domains switched back, but some did not, resulting in a remanent strain. It is also apparent that the overall strain in the 1st cycle for Sample A ($P \perp E$) is greater than that for Sample B ($P//E$). The reason behind this would be severe domain switching in Sample A, where the switching occurs into the transverse axis.

It should be pointed out that such a large strain in the beginning of the 1st cycle may also be affected by material damage, e.g., from the electrode and the matrix. Cao et al. have investigated the stress vs. strain relationship for PZT-based ferroelectric ceramics with copper foil ($t = 25$ μm) bonded between the ceramic plates [22]. They show stress–strain relations for the PZT ceramic and the copper foil where the stress–strain curve is different, depending on the material. This result suggests that stress vs. strain for our PZT samples can also be affected by the

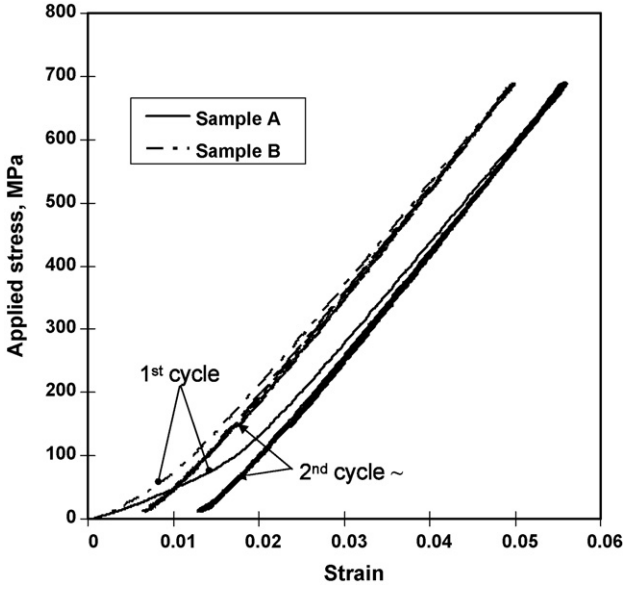

Fig. 2. Stress vs. strain relationship during the fatigue tests for Samples A and B.

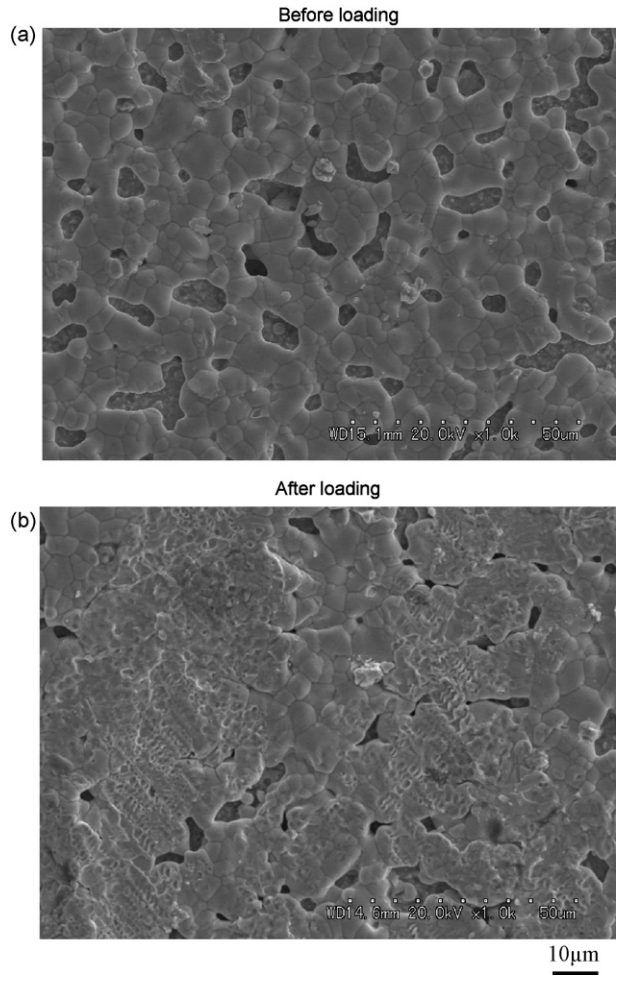

Fig. 3. SEM micrographs showing the surface of the plating before and after loading.

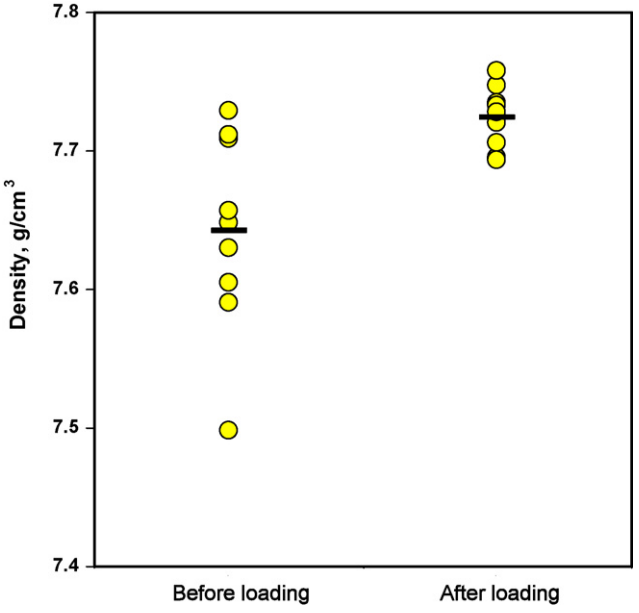

Fig. 4. Density of PZT ceramic before and after the applied load.

deformation caused by the silver electrode. Fig. 3 displays the SEM images of the electroplated layer before and after loading to about 140 MPa. In this case, the load was applied over the entire electrode of the sample. It is clear that pores are observed in the electrode before the mechanical load, but these have collapsed over a large area after loading. Note that the pores in the electrode might be created by the high temperature used in the firing process for electrode attachment [3]. We also determined the density of the PZT before and after loading to about 140 MPa with the results shown in Fig. 4. In this case, the sample density was determined by Archimedes' method. Although the data are scattered, it is important to note that the material density apparently increases after the loading process. From the above experiments, we consider that the large strain of the PZT ceram-

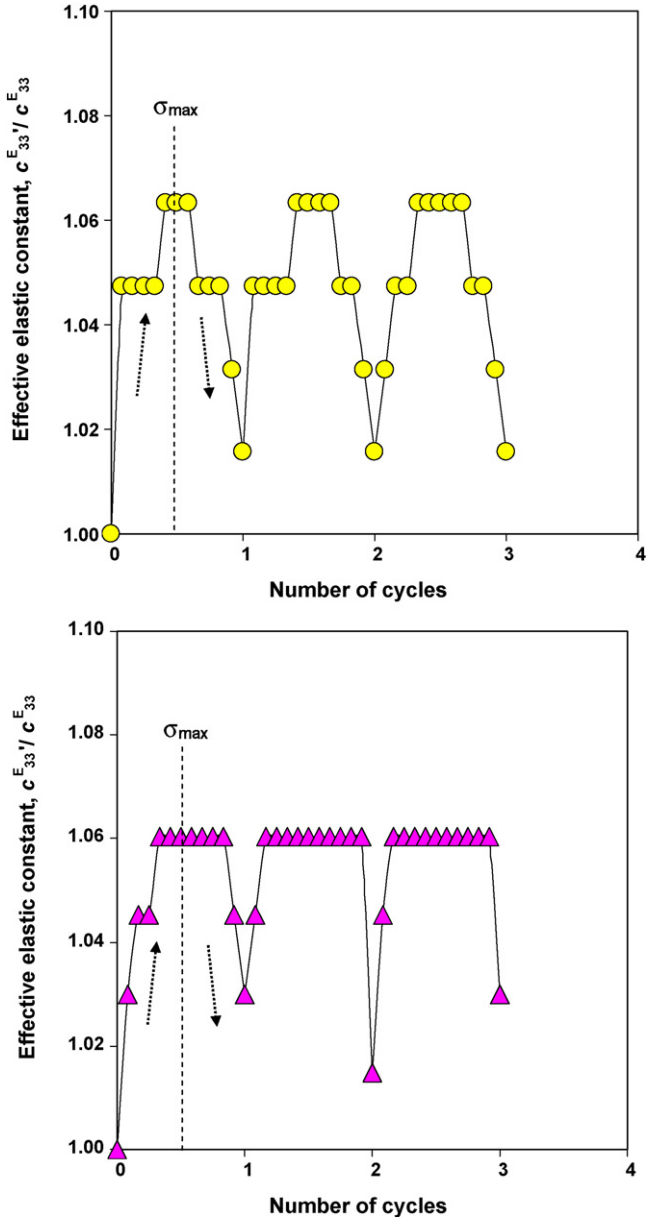

Fig. 5. Variation of the effective elastic constant of the PZT ceramics during cyclic loading (σ_{max} = 277.8 MPa) with different loading directions, Sample A vs. Sample B.

ics in the 1st cycle can play an important role in influencing the material characteristics.

3.2. Material properties

Fig. 5 shows the variation of the effective elastic constant as a function of the number of loading cycles for Samples A and B. Note that the effective elastic constant is relative to the initial effective elastic constant obtained after sample preparation (see Table 1), e.g., $c_{33}^{E'}/c_{33}^{E}$. It is seen that the $c_{33}^{E'}/c_{33}^{E}$ increases with increase of the applied load, then decreases with decrease of the load. The variations of effective elastic constant are almost the same for Samples A and B. This observation might suggest that the value of $c_{33}^{E'}$ cannot be influenced strongly by the loading direction. Fig. 6 shows the variation of the effective elastic constant as a function of the applied load in the 1st cycle. It should be noted that the load was applied at different maximum stress levels, e.g., σ_{max} 277.8 and 463 MPa. As with Fig. 5 the variation of $c_{33}^{E'}/c_{33}^{E}$ exhibits a concave shape for both samples, but the $c_{33}^{E'}/c_{33}^{E}$ data for the high stress sample (463 MPa) are greater than those for the low stress sample. This result can be attributed to the different severity of domain switching. Details of domain characteristics will be discussed in a later section of this paper.

Fig. 7 presents the variation of the electrical properties, including $c_{33}^{E'}/c_{33}^{E}$ (Fig. 6), as a function of the applied load in the 1st cycle. Compared to the results of effective elastic constant, the opposite sense of change of the electrical properties (electromechanical coupling coefficient, piezoelectric constant and permittivity) is obtained, in which the electrical properties are degraded with increase of the applied load. Such reduction in the electrical properties will be affected by the strain accumulation caused by the change of domain orientation during the

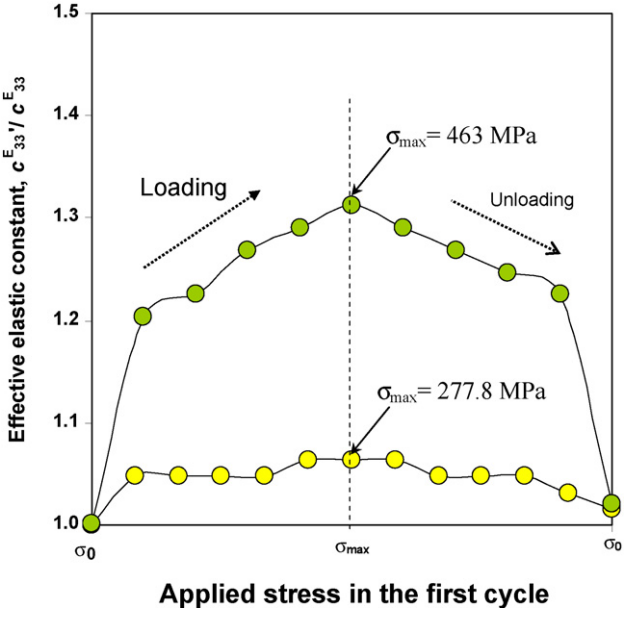

Fig. 6. Variation of the effective elastic constant of the PZT ceramics during a loading cycle (1 cycle) with different maximum stress (σ_{max} = 277.8 MPa and σ_{max} = 463 MPa) for Sample B.

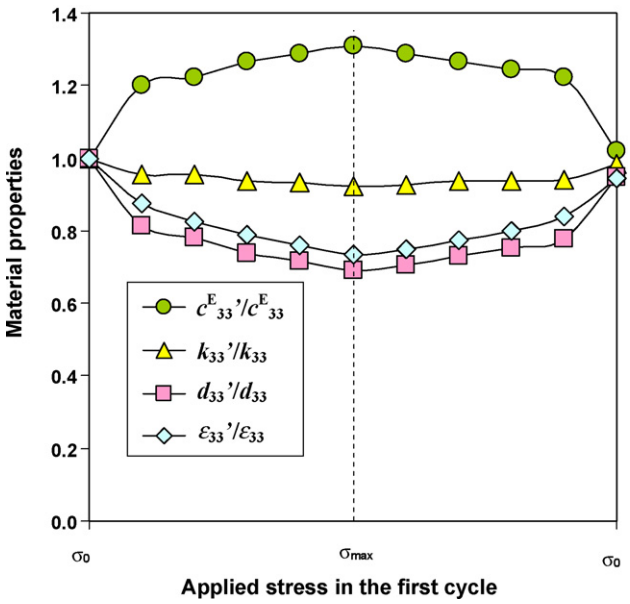

Fig. 7. Variation of the material properties of the PZT ceramics during a loading cycle (1 cycle, σ_{max} = 463 MPa) for Sample B.

loading process. In a prior study by Jones et al. [23], the strain accumulation during mechanical cycling was found to be time-dependent, because of the domain switching and they reported that the strain accumulation in PZT ceramics is truly a fatigue response.

To further examine the variation of material properties of PZT as a function of the number of cycles for Samples B and C, a fatigue test was conducted. The results obtained are shown in Fig. 8. In this approach, the specimen was cyclically loaded at σ_{max} 463 MPa, and the specimen fractured completely on the 15th cycle, as marked by X. It is clear that all material property variations for Sample C show a wave-like response, in which the effective elastic constant increases and electrical properties are degraded with increasing applied load. These results show a similar trend to the experimental data in Figs. 6 and 7. On the other hand, the degree of change of material properties decreases with increasing cycle number to final failure. This reduction may be caused by the material damage, e.g., microcrack. It also appears that the variations of the material properties for Sample B (in the 1st cycle) show a similar trend to those for Sample C. This result suggests that the thickness of the PZT sample may not influence the severe change of material properties.

3.3. Domain orientation

Because the PZT ceramic was considerably strained when loaded, the change of domain orientation, i.e., domain switching, might affect the material properties [24,25]. To verify this, the crystal structural orientation before and after loading was investigated. In this approach, a compressive load was conducted in a localized area (1 cm^2) of the sample surface with a load of about 5 kgf near the observation region. Fig. 9(a) displays an image quality map and Fig. 9(b) and (c) shows crystal orientation maps

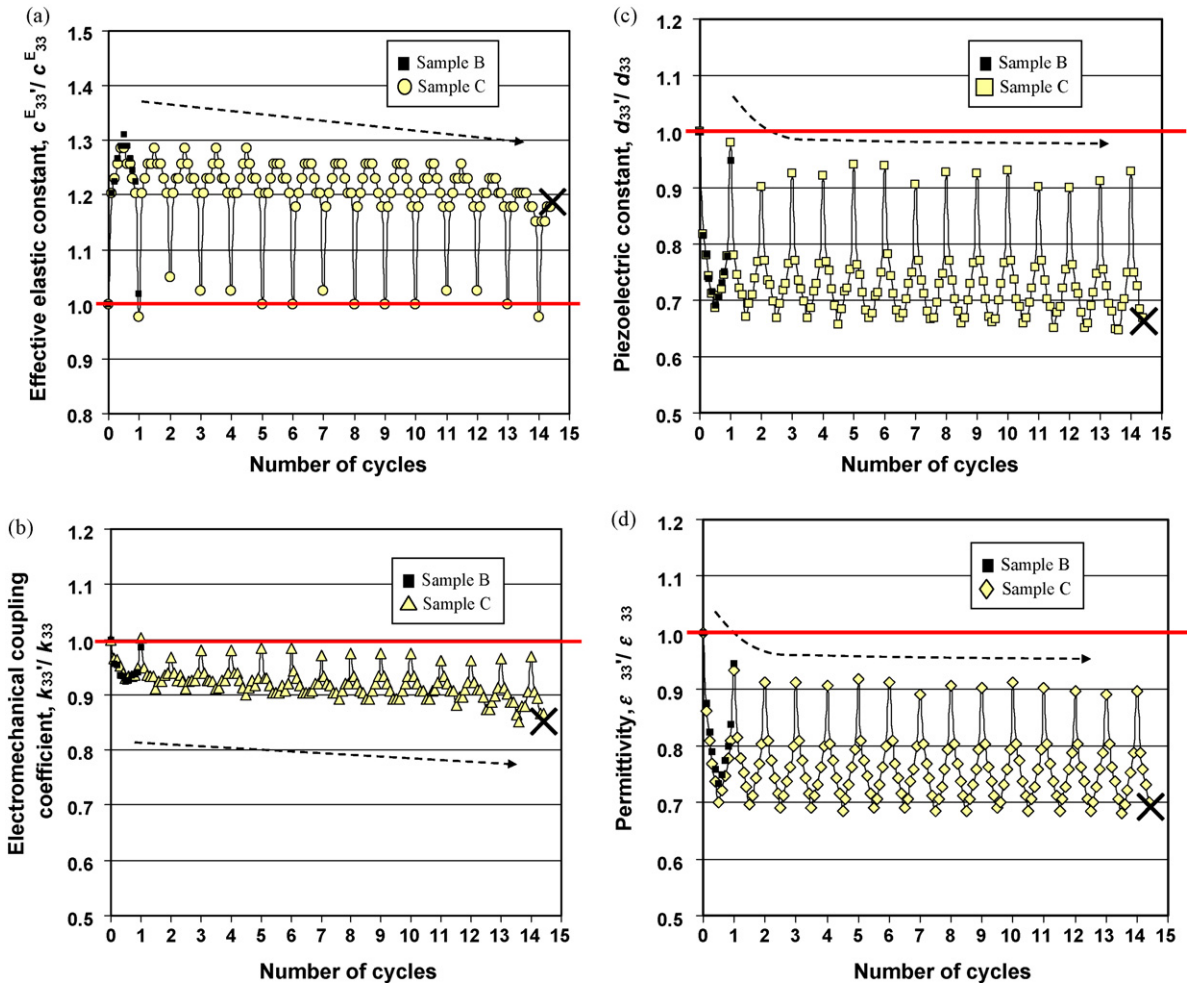

Fig. 8. Variation of the material properties of the PZT ceramics as a function of the number of cycles for Samples B and C (σ_{max} = 463 MPa): (a) c'^{E}_{33}/c^{E}_{33}; (b) k'_{33}/k_{33}; (c) d'_{33}/d_{33} and (d) $\varepsilon'_{33}/\varepsilon_{33}$.

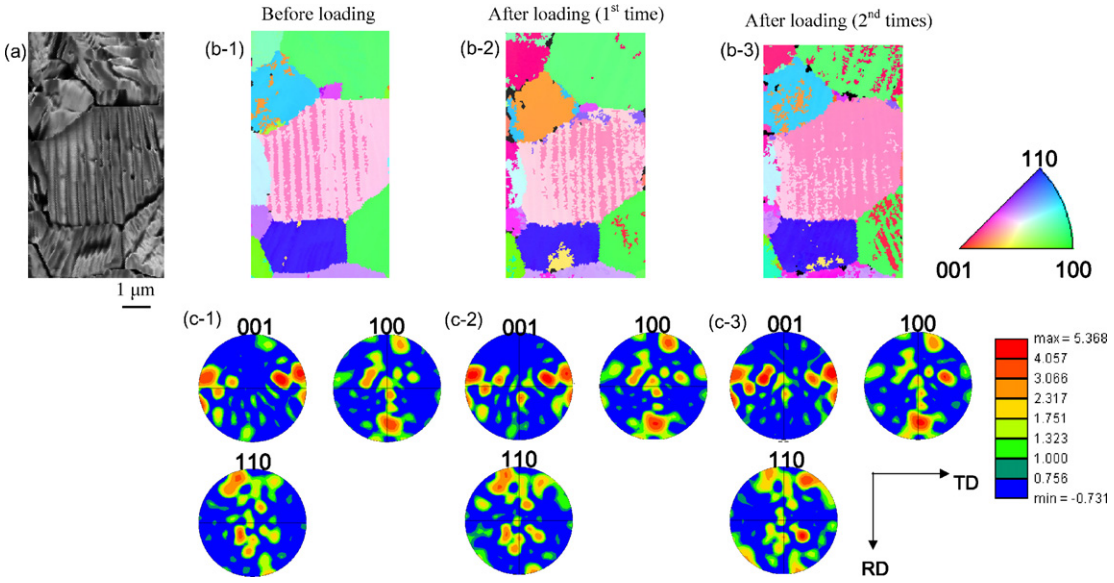

Fig. 9. EBSD analysis of the PZT ceramics before and after loading: (a) image quality map, (b) crystal orientation map and (c) the (0 0 1), (1 0 0) and (1 1 0) pole figures.

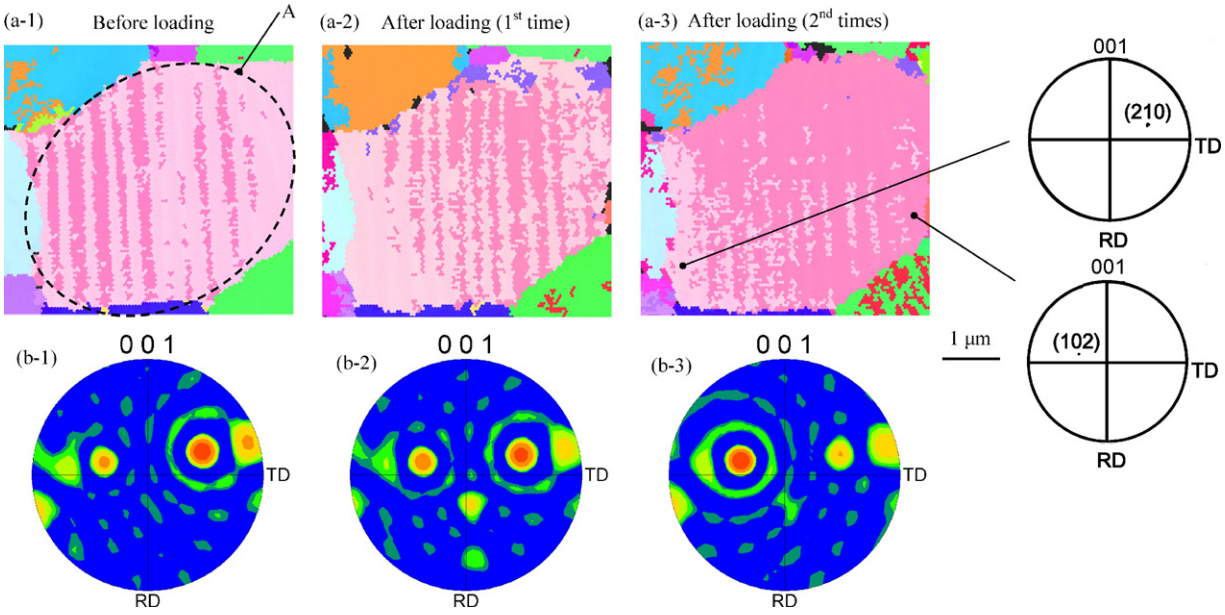

Fig. 10. EBSD analysis of grain A in the PZT ceramic before and after loading: (a) crystal orientation map and (b) the (0 0 1), (1 0 0) and (1 1 0) pole figures.

with their (0 0 1), (1 0 0) and (1 1 0) pole figures. The color level of each pixel in the crystal orientation map is defined according to the deviation of the measured orientation with respect to the ND direction (see the color key of the stereographic projection). From the EBSD analysis, the crystal orientation in the grains is different depending on the grain (see Fig. 9(b)). It is clear that the crystal orientation in some grains alters after the loading process, as shown by comparing Fig. 9(b-1) and (b-2), where about 90° domain switching occurs throughout. In addition, the domain switching zone increases on further loading, as shown by comparing the data for single loading Fig. 9(b-2) with that for two loadings Fig. 9(b-3). Fig. 10 also displays the domain orientation maps with the pole figures before and after loading in the grain (A), as enclosed by the dashed line. As can be seen, clear multiple domain switching occurs due to the applied load, in which the domain orientation changes from domain to domain by about 90° after the loading process [26]. For instance, the domain orientation in grain (A) is (2 1 0) before loading, but is tilted to (1 0 2) following the loading process. Similar 90° domain switching was obtained in the study by Jones [27]. He examined the domain orientation by X-ray diffraction, and demonstrated 90° domain switching in perovskite tetragonal ceramics through an intensity interchange between the 0 0 2 and 2 0 0 peaks.

It can be considered from the results of Figs. 9 and 10 that the asymmetry of 90° switching can cause strain accumulation in the sample [28]. Such an occurrence could support the formation of more severe internal stresses in the PZT ceramic, resulting in the high effective elastic constant, as shown in Fig. 6. Similar results were obtained in our previous work, in which the flexural modulus of the PZT ceramic was altered due to the change of lattice system from tetragonal to cubic [29]. Furthermore, it is expected the elastic modulus can be changed by domain wall motion although this cannot be revealed in the present work [28].

4. Conclusions

In situ measurements of the mechanical and electrical properties of PZT ceramics during loading to failure were carried out. On the basis of our results and discussion, the following conclusions can be drawn.

(1) The effective elastic constant increases with increasing mechanical load. This occurrence is affected by the strain accumulation arising from domain switching. In contrast, the effective elastic constant decreases with increasing numbers of cycles, due to material damage.
(2) Domain switching occurs when the load is applied directly to the sample. In this, the crystal orientation alters from domain to domain by 90° throughout some grains. The 90° domain switching can occur anywhere in the sample.
(3) The electrical properties (k_{33}, d_{33} and ε_{33}) decrease with increasing applied load, which is opposite sense of the change of effective elastic constant. The reduction in the material properties is caused by the internal strain.
(4) The material properties (c_{33}^{E}, k_{33}, d_{33} and $\varepsilon_{33}/\varepsilon_0$) decrease with increasing numbers of cycles to final fracture. This can be affected by material damage, e.g., micro-crack. There are no clear effects due to the poling direction or sample thickness on the material properties during the applied loading.

Acknowledgements

The authors would like to sincerely appreciate many experimental supports by Mr. Kunihiro Funatsu and Mr. Kazuto Sato. The authors would also like to express the appreciation to Mr. Hiroshi Tojo for his technical supports. Additional support from Ms. Miho Sato and Ms. Noriko Muro is gratefully acknowledged.

References

[1]. Oates WS, Lynch CS, Lupascu DC, Njiwa ABK, Aulbach E, Rödel J. Subcritical crack growth in lead zirconate titanate. *J Am Ceram Soc* 2004;**87**:1362–4.

[2]. Nuffer J, Lupascu DC, Rödel J. Damage evolution in ferroelectric PZT induced by dipolar electric cycling. *Acta Mater* 2000;**48**:3783–94.

[3]. Okayasu M, Aoki S, Mizuno M. Effects of silver-based metal electroplate on fatigue properties of PZT ceramics. *Int J Fatigue* 2008;**30**:1115–24.

[4]. Cheng BL, Reece MJ, Guiu F, Algueró M. Fracture of PZT piezoelectric ceramics under compression–compression loading. *Scr Mater* 2000;**42**:353–7.

[5]. Pojprapai(Imlao) S, Jones JL, Hoffman M. Domain switching under cyclic mechanical loading in lead zirconate titanate. *J Am Ceram Soc* 2005;**89**:3567–9.

[6]. Jones JL, Hoffman M, Vogel SC. Ferroelastic domain switching in lead zirconate titanate measured by in situ neutron diffraction. *Mech Mater* 2007;**39**:283–90.

[7]. Li F, Li S, Fang D. Domain switching in ferroelectric single crystal/ceramics under electromechanical loading. *Mater Sci Eng B* 2005;**120**:119–24.

[8]. Kreher WS. Influence of domain switching zones on the fracture toughness of ferroelectrics. *J Mech Phys Solids* 2002;**50**:1029–50.

[9]. Shrout TR, Zhang SJ. Lead-free piezoelectric ceramics: alternatives for PZT? *J Electroceram* 2007;**19**:111–24.

[10]. Pojprapai(Imlao) S, Jones JL, Studer AJ, Russell J, Valanoor N, Hoffman M. Ferroelastic domain switching fatigue in lead zirconate titanate ceramics. *Acta Mater* 2008;**56**:1577–87.

[11]. Hatanaka T, Hasegawa H. Observation of domain structures in tetragonal $Pb(Zr_xTi_{1-x})O_3$ single crystals by chemical etching method. *Jpn J Appl Phys* 1992;**31**:3245–8.

[12]. Kohli M, Muralt P, Setter N. Removal of 90° domain pinning in (1 0 0) $Pb(Zr_{0.15}Ti_{0.85})O_3$ thin films by pulsed operation. *Appl Phys Lett* 1998;**72**:3217–9.

[13]. Anteboth S, Brückner-Foit A, Hoffmann MJ, Sutter U, Schimmel Th, Müller M. Electromechanical behaviour of PZT with real domain structure. *Comput Mater Sci* 2008;**41**:420–9.

[14]. Al-Danaf EA. Texture evolution and fraction of favorably oriented fibers in commercially pure aluminum processed to 16 ECAP passes. *Mater Sci Eng A* 2008;**292**:141–52.

[15]. McNelley TR, McMahon ME. Microtexture and grain boundary evolution during microstructural refinement processes in Supral 2004. *Metall Mater Trans A* 1997;**28**:1879–87.

[16]. Yoda R, Nakazawa S, Onishi T. Application of an electron backscatter diffraction pattern to Cu damascene-fabricated interconnections filled by a high-pressure anneal process. *J Electron Mater* 2002;**31**:16–22.

[17]. Fuji Ceramics Co., *Piezoelectric Ceramics: Technical Handbook* (Fuji Ceramics Co.).

[18]. Mizuno M, Odagiri N, Okayasu M. Variation of material properties of piezoelectric ceramics due to electric loading evaluated by resonance frequency. *Key Eng Mater* 2007;**345–346**:1521–4.

[19]. Randle V. *Microtexture Determination and its Applications*. 2nd ed. London: Money; 2003.

[20]. Calderon-Moreno JM, Popa M. Stress dependence of reversible and irreversible domain switching in PZT during cyclic loading. *Mater Sci Eng A* 2002;**336**:124–8.

[21]. Cao H, Evar A. Nonlinear deformation of ferroelectric ceramic. *J Am Ceram Soc* 1993;**76**:890–6.

[22]. Cao HC, Graef MD, Evans AG. Structure and properties at the ferroelectric/electrode interface between lead zirconate titanate and copper. *J Am Ceram Soc* 1993;**76**:3019–23.

[23]. Jones JL, Salz CRJ, Hoffman M. Ferroelastic fatigue of a soft PZT ceramic. *J Am Ceram Soc* 2005;**88**:2788–92.

[24]. Okayasu M, Odagiri N, Mizuno M. Damage characteristics of lead zirconate titanate piezoelectric ceramic during cyclic loading. *Int J Fatigue* 2009;**31**:1434–41.

[25]. Okayasu M, Ozeki G, Mizuno M. Fatigue failure characteristics of lead zirconate titanate piezoelectric ceramics. *J Eur Ceram Soc* 2009;**30**:713–25.

[26]. Kimachi H, Tsunekawa T, Shirakihara K, Tanaka K. Observation of crystal orientation, domain and domain switching in ferroelectric ceramics by EBSP method. *J Jpn Foundry Eng Soc* 2008;**74**:335–41 [in Japanese].

[27]. Jones JL. The use of diffraction in the characterization of piezoelectric materials. *J Electroceram* 2007;**19**:67–79.

[28]. Jones JL, Hoffman M. R-curve and stress–strain behavior of ferroelastic ceramics. *J Am Ceram Soc* 2006;**89**:3721–7.

[29]. Okayasu M, Otake M, Bitoh T, Mizuno M. Temperature dependence of the fatigue and mechanical properties of lead zirconate titanate piezoelectric ceramics. *Int J Fatigue* 2009;**31**:1254–61.